World Journal of Microbiology and Biotechnology (2025) 41:182
https://doi.org/10.1007/s11274-025-04413-8

RESEARCH

Pyrrolnitrin is integral for antimicrobial activity and phenazine biosynthesis of *Pseudomonas chlororaphis* strains

Mahnoor Zameer[1] · Izzah Shahid[2] · Deeba Noreen Baig[1] · Roman Makitrynskyy[3] · Kauser Abdulla Malik[1] · Andreas Bechthold[3] · Samina Mehnaz[1]

Received: 22 December 2024 / Accepted: 14 May 2025

Abstract

Pseudomonas species are recognized for producing a diverse array of microbial metabolites with significant potential across various fields. Pyrrolnitrin (PRN), a halogenated metabolite based on phenylpyrrole, exhibits potent antibiotic properties. This research aimed to examine the influence of pyrrolnitrin on the antagonistic properties of *Pseudomonas chlororaphis* strains PB-St2, FS2, and RP4. Mutants of *P. chlororaphis* were generated by inhibiting *prn*A using two distinct suicide vectors, pEX18Tc and pKC1132. Analysis via high performance liquid chromatography (HPLC) revealed that pyrrolnitrin production was completely eliminated in the pKC1132 mutant and decreased by 82.5% in the pEX18Tc mutant. Both mutants also exhibited reduced phenazine production, with pKC1132 mutants showing a 61.1% reduction in phenazine-1-carboxylic acid (PCA) and pEX18Tc-induced mutants displaying a 39.9% decrease in PCA. To further elucidate the dependence of pyrrolnitrin production on other regulatory elements, the complete *prn*ABCD operon with its native promoter was cloned and expressed in *Escherichia coli* (BL21). The antimicrobial potential of purified pyrrolnitrin was evaluated against fungal plant pathogens, human bacterial pathogens, and cancer cell lines (HepG-2 and SF767). The most pronounced inhibitory effect on *Alternaria alternata* was observed with 100 µg of pyrrolnitrin, resulting in an 82% reduction in spore formation followed by its effect on *Aspergillus niger*, causing a 75% decrease in spore production. Pyrrolnitrin's antibacterial activity produced inhibition zones of 1.8 cm against *Salmonella enterica*, 3.4 cm against *Bacillus cereus*, and 1.4 cm against *Staphylococcus* sp. at a concentration of 75 µg. The antiproliferative effects of pyrrolnitrin on cancer cell lines demonstrated 50% inhibition of both HepG-2 and SF767 cell lines at concentrations of 15 µg and 25 µg, respectively. Pyrrolnitrin exhibited significant antifungal and antibacterial activities, as well as cytotoxic effects on cancer cell lines, indicating its potential as both a biocontrol agent and therapeutic compound.

Keywords Antimicrobial · Anticancer · *Pseudomonas chlororaphis* · Pyrrolnitrin

Introduction

Phenylpyrroles have been reported as efficacious agents against various fungal and bacterial phytopathogens (Abd El-Hameed et al. 2021). Among pyrroles, pyrrolnitrin [3-chloro-4-(2-nitro-3-chlorophenyl) pyrrole] belongs to a class of phenylpyrrole halo-metabolites predominantly produced by Gram-negative bacteria (Schmidt et al. 2009). Structurally, pyrrolnitrin (PRN) comprises benzene and pyrrole rings ($C_{10}H_6O_2N_2Cl_2$, MW: 257.07 g/mol melting point: 124.5 °C) with two chlorine atoms and a nitro group (van Pée and Ligon 2000). The biosynthesis process of pyrrolnitrin involves a series of enzymatic reactions governed by the *prn*ABCD gene cluster. The initial step is catalyzed by tryptophan halogenase (*prn*A), which converts tryptophan

✉ Samina Mehnaz
saminamehnaz@fccollege.edu.pk

1 Kauser Abdulla Malik School of Life Sciences, Forman Christian College (A Chartered University), Ferozepur Road, Lahore 54600, Pakistan

2 Institute of Multidisciplinary Research in Applied Biology, Public University of Navarra, Campus Arrosadia, Pamplona 31006, Spain

3 Institute for Pharmaceutical Biology and Biotechnology, University of Freiburg, Stefan-Meier-Str. 19, 79104 Freiburg, Germany

Published online: 26 May 2025

into 7-chlorotryptophan. Subsequently, aminotransferase (*prn*B) transforms this compound into 7-chlorokynurenine. The next stage involves the reduction of this intermediate to 7-chlorohydroxyindole, facilitated by the reductase enzyme encoded by *prn*C. The final step in the synthesis is performed by the halogenase (*prn*D), which incorporates a halogen group to produce pyrrolnitrin (Singh et al. 2016).

Pyrrolnitrin was initially isolated from *Pseudomonas pyrrocinia*, and later reported in various fluorescent and non-fluorescent *Pseudomonas* species. Subsequently, multiple strains of other bacteria, including *Burkholderia cepacia*, *Corallococcus exiguus*, *Cystobacter ferrugineus*, *Enterobacter agglomerans*, *Myxococcus fulvus*, *Serratia* spp., and *Actinosporangium vitaminophilum*, were found to produce pyrrolnitrin in varying quantities. *Serratia plymuthica* and *S. ruhidaea* have been identified as enhanced pyrrolnitrin producers. A recent investigation identified a strain from the *B. cepacia* complex, JKB9, which demonstrates broad-spectrum antifungal activity. This strain was observed to inhibit the growth of several plant pathogens, including *Phytophthora capsici*, *Fusarium oxysporum*, and *Rhizoctonia solani* (Jung et al. 2018; Mohamed et al. 2020; Zhang et al. 2020a, b, c, d).

Among the Gram-negative bacteria, *Pseudomonas* spp. have been documented as the main producer of pyrrolnitrin which significantly add to their fungicidal potential. As an example, a strain of *P. chlororaphis* G05 lacking phenazine production (*phz* knockout) demonstrated effective suppression of fungal plant pathogens, such as *F. graminearum*, *Colletotrichum gloeosporioide*, and *Botrytis cinerea*. This inhibitory effect was attributed to the strain's capacity to synthesize pyrrolnitrin (Huang et al. 2018). Likewise, enhanced biocontrol efficacy against wheat and canola fungal pathogens (*Pythium ultimum*, *Rhizoctonia solani*, *Gaeumannomyces graminis var. tritici*) was achieved by *P. synxantha* 2–79 strain transformed with pyrrolnitrin synthesis genes (Zhang et al. 2020a, b, c, d). Similarly, pyrrolnitrin was the main antifungal compound of *P. protegens* strain W45 responsible for the inhibition of *Sclerotinia sclerotiorum* (Bajpai et al. 2018). Pyrrolnitrin was also one of the most abundant antibiotics produced by *P. protegens* FD6 (Zhang et al. 2020a, b, c, d). However, despite the considerable contribution of pyrrolnitrin, phenazines are still considered the primary antifungal compounds, particularly among fluorescent species of *Pseudomonas*. Furthermore, due to its lower yield compared to phenazines, this metabolite is rarely isolated in pure form. Consequently, there are only a few examples where its expression in heterologous systems has been studied (Schmidt et al. 2009). Besides, several regulatory mechanisms have been documented for the differential suppression or upregulation of pyrrolnitrin and phenazines. For instance, some *Pseudomonas* spp. can repress pyrrolnitrin synthesis to upscale the production of phenazines. Such as, *P. chlororaphis* G05, a TetR/AcrR family regulator *pip* promoted the production of phenazines while inhibited the synthesis of pyrrolnitrin (Yu et al. 2021). Similarly, *P. chlororaphis* G05 has also shown the significance of LysR-type transcriptional regulator *Fin*R in regulation of pyrrolnitrin synthesis (Chen et al. 2021). Nevertheless, the relationship between the phenazine and pyrrolnitrin pathways, as well as its impact on the overall antifungal efficacy of *Pseudomonas* strains lacking pyrrolnitrin production, remains poorly understood. This study aimed to investigate the effects of pyrrolnitrin-deficient mutants of *P. chlororaphis* strains PB-St2, FS2, and RP4 on their antifungal properties, as well as to examine the functionality of the pyrrolnitrin gene cluster in heterologous systems for enhanced production. Additionally, the study sought to examine pyrrolnitrin's potential as both an antibacterial and anticancer agent.

Materials and methods

Microbial strains, plasmids and growth conditions

The microbial strains and plasmids used in the present study are listed in Table 1. Previously characterized *Pseudomonas* strains PB-St2, FS2 and RP4 (Shahid et al. 2017; Mehnaz et al. 2014) were maintained on nutritionally defined Kings' B medium (KB; King et al. 1954) at 28 °C. Mutated *Pseudomonas* strains were cultured on KB medium augmented with selective antibiotics corresponding to the plasmid utilized. Such as, mutants harboring pKCPN plasmid were sustained on KB supplemented with apramycin (50 µg/mL), and mutants with pEXPN were maintained on KB supplemented with tetracycline (30 µg/mL). Various strains of *E. coli* were cultivated in Luria Bertani (LB; Bertani 1952) medium at 37 °C with the addition of selective antibiotics corresponding to the plasmids; PBpSK-1, FSpSK-2, RPpSK-3 with ampicillin (100 µg/mL). Fungal phytopathogens were cultivated on potato dextrose agar (PDA) and maintained at 25 °C.

Characterization and purification of Pyrrolnitrin

P. chlororaphis strains PB-St2, RP4, and FS2 were cultivated in King's B broth, with each 100 mL of medium containing 1% (v/v) primary inoculum, 0.61 g/L tryptophan, and 2% glucose, for five days at 28 °C. Cultures were harvested at 3234 × *g* for 15 min (HERMLE Z 513 K Centrifuge, Germany), supernatants were acidified with HCl (pH 2.0), and extracted with equal volume of ethyl acetate. The pellets were suspended in 30 mL acetone, sonicated, dried using a rotary evaporator (Buchi 210R, Germany)

Table 1 List of microbial strains and plasmids used in this study

Strains/ Plasmids	Relevant Characteristics	Source/Accession Number
Wild type Pseudomonas strains		
PB-St2	Wild type: *Pseudomonas chlororaphis* subsp. *aurantiaca*; *prn*$^{+}$	Lab collection, 16 S rRNA; EU761590 Complete Genome; AYUD00000000 Mehnaz et al. (2014)
FS2	Wild type: *Pseudomonas chlororaphis* subsp. *aurantiaca*; *prn*$^{+}$	Lab collection, 16 S rRNA; LN898137 Shahid et al. (2017)
RP4	Wild type: *Pseudomonas chlororaphis* subsp. *chlororaphis*; *prn*$^{+}$	Lab collection, 16 S rRNA; KT888010 Shahid et al. (2017)
Mutants of *Pseudomonas* strains		
ΔPKC-A	A mutant of PB-St2 derived by pKCPN; Apr^{R}, *prn*$^{-}$	This study
ΔFKC-A	A mutant of FS2 derived by pKCPN; Apr^{R}, *prn*$^{-}$	This study
ΔRKC-A	A mutant of RP4 derived by pKCPN; Apr^{R}, *prn*$^{-}$	This study
ΔPPX-T	A mutant of PB-St2 derived by pEXPN; Tet^{R}, *prn*$^{-}$	This study
ΔFPX-T	A mutant of FS2 derived by pEXPN; Tet^{R}, *prn*$^{-}$	This study
ΔRPX-T	A mutant of RP4 derived by pEXPN; Tet^{R}, *prn*$^{-}$	This study
E. coli		
DH10β	A host strain for cloning	Dr. Harald Gross´s lab, University of Tubingen
BL21 (DE3)	A host strain for expression	Dr. Harald Gross´s lab, University of Tubingen
Fungal phytopathogens		
CF	*Colletotrichum falcatum*	Lab collection/PP663265
FS	*Fusarium incarnatum*	Lab collection/MN636869
AN	*Aspergillus niger*	Lab collection/PP663271
AA 1	*Alternaria alternata*	Lab collection/OP740511
AA 2	*Alternaria alternata*	Lab collection/OP740510
Bacterial pathogens		
BCi	*Bacillus cereus*	Lab collection/MZ414206
SLi	*Salmonella enterica*	Lab collection/MZ414205
KOi	*Klebsiella* sp.	Lab collection/MZ414202
PAi	*Pseudomonas aeruginosa*	Lab collection/OP740518
STi	*Staphylococcus* sp.	Lab collection/LT221185
Plasmids		
pBSK(-)	pBluescript SK (-); standard cloning vector, T7 promoter, orientation of MCS allows rescue of antisense strand ssDNA, *amp*^{R}	Dr. Harald Gross´s lab, University of Tubingen
pEX18Tc	A broad-host-range, Flp-FRT recombination system for site-specific excision of chromosomally-located DNA sequences; *tet*^{R}	Dr. Harald Gross´s lab, University of Tubingen
pKC1132	Suicide vector that can be used for cloning and homologous recombination experiments; *apr*^{R}	Dr. Bechthold's lab, University of Freiburg
Constructs		
PBpSK-1	*prn*ABCD operon from PB-ST2 with its promoter region cloned in pBSK(-)	This study
FSpSK-2	*prn*ABCD operon from FS2 with its promoter region cloned in pBSK(-)	This study
RPpSK-3	*prn*ABCD operon from RP4 with its promoter region cloned in pBSK(-)	This study
pKCPN	*prn*A region cloned in pKC1132	This study
pEXPN	*prn*A region cloned in pEX18Tc	This study
Heterologous clones		
PBP1	PBpSK-1 transformed in BL21	This study
FBP2	FSpSK-2 transformed in BL21	This study
RBP3	RPpSK-3 transformed in BL21	This study

and resuspended in 5 mL methanol. Crude extracts were subjected to thin-layer chromatography (TLC) using Silica Gel 60 F_{254} (20 × 20 cm, Merck, Germany) plates and mobile phase *n*-hexane: ethyl acetate (2:1). Purple spots, indicative of pyrrolnitrin presence, were identified on the plates after staining with a 2% Ehrlich Reagent comprising 2% p-dimethyl amino benzaldehyde with 10 N sulfuric acid (de Souza and Raaijmakers 2003; Costa et al. 2009). The

Table 2 HPLC run time and mobile phase for the assessment of Pyrrolnitrin fractions

Time (minutes)	Water % (Solvent A)	Acetonitrile % (Solvent B)
0.0	95	5
1.0	95	5
15.0	5	95
30.0	5	95

retardation factor (*Rf*) for each separated spot was calculated using the standard formula by comparing with standard as mentioned by Jung et al. (2018).

Pyrrolnitrin (PRN) spots on TLC plates were scraped and dissolved in methanol for further analysis. The samples were purified by high-performance liquid chromatography (HPLC) on Waters HPLC System (e2995, Separations Module) coupled with 2998 photodiode-array (PDA) detector using a Nucleosil C18 column (4.6 × 250 mm, 5µM; Macherey-Nagel, Germany) using the water and acetonitrile mobile phase (Table 2). The total HPLC runtime was 30 min, and the flow rate was set at 1.0 mL/min. To minimize variation in quantification, samples were taken in triplicate and compared against the pyrrolnitrin standard (Sigma Aldrich). Purified fractions were sent to TTI Testing Laboratories Lahore (commercial facility) for liquid-chromatography mass spectrometry (LCMS) validation.

Antimicrobial activities of purified Pyrrolnitrin

The disk-diffusion method was employed to assess the antifungal efficacy of purified pyrrolnitrin against various fungal phytopathogens, including *Fusarium solani*, *Colletotrichum falcatum*, *Alternaria alternata*, and *Aspergillus niger*. Potato dextrose agar plates were inoculated with fungal suspensions of each pathogen, containing 10^4 spores/mL. Filter paper discs (6 mm in diameter), sterilized and loaded with 100 µg of pyrrolnitrin, were placed on these inoculated plates (Soliman et al. 2022). Methanol-treated discs served as a negative control. Following a 5-day incubation period at 25 °C, hyphal de-morphogenesis was examined using both stereo and fluorescent microscopes at 40X magnification (Olympus IX83). Spore quantification was performed using a hemocytometer at 100X magnification.

Antibacterial properties of pyrrolnitrin were evaluated against four bacterial pathogens: *Bacillus cereus*, *Pseudomonas aeruginosa*, *Salmonella enterica*, *Staphylococcus* sp. and *Klebsiella oxytoca*. The bacteria were grown overnight in 10 mL of LB broth at 37 °C. Subsequently, 20 µL of each bacterial culture was plated on LB agar plates in triplicate and filter paper discs loaded with varying concentrations of pyrrolnitrin (10, 15, 25, 50, 75, and 100 µg/mL) were seeded on the inoculated plates. Plates were incubated for 48 h at 37 °C and observed for the presence of halo-zones around the discs (Hemeg et al. 2020).

Table 3 Primers used for the amplification of Pyrrolnitrin Operon from *Pseudomonas* strains

Primers	Sequence	Restriction Site
*prn*_op_F	5′-AAA*tctaga*GCTGTTCGTCAAGGAATGG-3′	*Xba*I
*prn*_op_R	5′-AAA*ggatcc*TGCAACAGCCAGATAGTCATG-3′	*Bam*HI
Δ*prn*F	5′-AAA*tctaga*GTGGTCGACGAGGTCGTG-3′	*Xba*I
Δ*prn*R	5′-AAA*gatatc*GGAAGTGCTTCACCAGGTG-3′	*Eco*RV

Anticancer activity

The cytotoxic effects of various pyrrolnitrin concentrations (10, 15, 25, 50, 75, and 100 µg/mL) were evaluated on two cancer cell lines: HepG-2 (human liver cancer) and SF767 (glial cells from the central nervous system). The assessment utilized the 3-(4,5-Dimethylthiazol-2-yl)-2,5-Diphenyltetrazolium Bromide (MTT) bioassay following the method outlined in Zameer et al. (2025). Each experiment was conducted twice, and the results were obtained using an ELISA reader (Bio-Rad, I-Mark, USA) at 595 nm wavelength.

Heterologous expression via cloning in *E. coli* BL21

The complete nucleotide sequence of the pyrrolnitrin operon was obtained from the genome sequence data of PB-St2 available at NCBI (Accession Number: AYUD00000000, Mehnaz et al. 2014). The complete *prn*ABCD operon was found within the genomic region of 3,809,329–3,815,480. Using Primer 3 (Koressaar et al. 2018) and Primer-BLAST (https://www.ncbi.nlm.nih.gov/tools/primer-blast/), two sets of primers were designed: one targeting the entire operon with its native promoter and another targeting a portion of the *prn*A gene (Table 3). Gene-specific primers *prn*ABCD F/R were utilized to amplify the entire pyrrolnitrin operon region, including its native promoter, from each *Pseudomonas* strain. Genomic DNA of each strain was extracted using a GeneJet Genomic DNA Purification Kit (K0721, Thermo Scientific, USA). The PCR reaction mixture (50 µL), was composed of the following: 25 µL Taq plus buffer (2X, Thermo Scientific), 2 µL dNTPs (2.5 mM), 5 µL DMSO (100%), 1 µL Phusion enzyme (2 U/µL, Thermo Scientific), 4 µL Phusion HF buffer (5X, Thermo Scientific), 1 µL each of forward and reverse primers (20 pmol), 2 µL template DNA (>400 ng/µL), and 9 µL ddH_2O. PCR conditions followed were: initial denaturation (95 °C) for 3 min, followed by 35 cycles of denaturation (92 °C) for 30 s, annealing and

extension (62 °C) for 4 min (40 s/Kb), and final extension (72 °C) for 10 min. The PCR product was resolved on a 0.8% agarose gel and purified using the GeneJet PCR Purification Kit (K0702, Thermo Scientific, USA). The Phusion enzyme was used to create blunt ends in the PCR product, while pBluescript (-) was digested with *Eco*RV to generate compatible ends. This was performed to ligate both the PCR product and plasmid seamlessly via blunt-end ligation. Ligation was conducted using ligase (1 U/µL) in a 20 µL reaction, incubated overnight at 16 °C to yield PBpSK-1, FSpSK-2, and RPpSK-3 constructs (Hao et al. 2019). Constructs were validated using SnapGene (https://www.snapgene.com/plasmids).

Electrocompetent cells of *E. coli* (BL21) were prepared following the protocol of Gonzales et al. (2013) with modifications. Initially, a small aliquot (1%) of the primary culture was inoculated into 100 mL of LB broth and incubated until the optical density at 600 nm reached 0.5–0.6. The cells were subsequently harvested by centrifugation at 3234×*g* for 10 min at 4 °C. The harvested cells were subjected to two washing cycles with chilled, autoclaved distilled water, followed by an additional wash using a 10% glycerol solution. Subsequently, the cell pellet was resuspended in 1 mL of cold 10% glycerol. The resultant suspension was aliquoted into 100 µL portions and stored at -80 °C for future use.

The constructs (pBpSK-1, fSpSK-2, and rPpSK-3) were transformed into the electrocompetent BL21 cells to generate PBP1, FBP2, and RBP3 clones. For transformation, 5 ng of each construct was individually transformed to a 100 µL aliquot of competent cells, transferred to chilled electroporation cuvette (BioRAD) and subjected to a voltage shock of 2 KV. The volume was increased to 1 mL with 950 µL of sterile broth and incubated for 1 h. A 100 µL fraction from each aliquot was spread on LB plates supplemented with 100 µg ampicillin, 40 µL X-Gal (20 mg/mL), and 40 µL IPTG (100 mM), and incubated at 37 °C overnight (Liu et al. 2014). White colonies were randomly selected for plasmid isolation.

To confirm the presence of the entire operon, a restriction digestion was performed, followed by a 2-h incubation at 37 °C. The reaction mixture, totaling 20 µL, consisted of plasmid (10 µL; 150–200 ng), Tango buffer (2 µL; 2×, Thermo Scientific), enzyme (1 µL; 1 U/µL, Thermo Scientific), and distilled water (7 µL). This mixture was incubated at 37 °C for 1 h for single digestion, and 2 h for double digestion. Sequencing (Macrogen, Republic of Korea) was used to ultimately validate the constructs from each host strain. The antifungal activity of these heterologous clones was evaluated using the disc diffusion assay as previously described.

Construction of knockdown mutant strains

To knockdown the expression of *prn*ABCD operon, two disruption plasmids, pEXPN and pKCPN, were generated using two different suicide vectors, pEX18Tc and pKC1132. A 540 bp fragment encoding part of tryptophan halogenase (*prn*A) gene was amplified using *Δprn*F/R primers (Table 3, Fig. S1). The reverse complement sequence of the target site was inserted into the plasmid to ensure 5′ to 3′ complementarity and antisense RNA hybridization to the target mRNA (Ji et al. 2017). The 50 µL reaction mixture contained 25 µL Taq plus mix, 2 µL each of forward and reverse primers (20 pmol), 4 µL template DNA (> 400 ng/µL), and 17 µL d.H_2O. PCR steps included initial denaturation (95 °C) for 5 min, followed by 35 cycles of second denaturation (92 °C) for 30 s, annealing (62 °C) for 30 s, extension (72 °C) for 1 min 30 s, and final extension (72 °C) for 10 min. Through primers, restriction sites of *Xba*I and *Eco*RV were introduced into the PCR product. Later, the PCR product was digested with *Xba*1 and *Eco*RV, pEX18Tc with *Sma*I-*Xba*I, and pKC1132 with *Eco*RV-*Xba*I and incubated at 37 °C for 3 h. The purified PCR product was ligated to pEX18Tc to generate pEXPN, and pKC1132 to generate pKCPN. Construction was confirmed by restriction digestion and sequencing. The constructs were transformed into electrocompetent cells of *Pseudomonas* strains PB-St2, FS2 and RP4. A 100 µL aliquot of transformed cells was spread on antibiotic selection plates and incubated overnight at 28 °C. Kings' B agar plates containing apramycin (50 µg/mL) were used to select mutants derived by pKCPN construct, and tetracycline (30 µg/mL)-supplemented plates were used to select pEXPN derived mutants (Hao et al. 2019).

Evaluation of antifungal effect of Pyrrolnitrin knockdown *Pseudomonas* strains against fungal phytopathogens

To confirm the production of pyrrolnitrin in clones and its absence in knockdown mutants, extracts of constructs and knockdown strains were subjected to HPLC and TLC analysis. Extracts were prepared using the method outlined in Sect. 2.2 and examined for the presence or absence of pyrrolnitrin bands on Silica Gel 60 F254 plates. The mobile phase used was *n*-hexane: ethyl acetate. As a control, extracts from wild type *P. aurantiaca* strains (PB-St2, RP4, FS2) were utilized, while purified pyrrolnitrin fractions served as the standard. All the extracts were analyzed on HPLC based on the profile mentioned in Table 2. Antifungal activities of synthesized clones and pyrrolnitrin knockdowns were assessed using disc-diffusion bioassay against fungal phytopathogens as mentioned in the section (Antimicrobial activities of purified pyrrolnitrin).

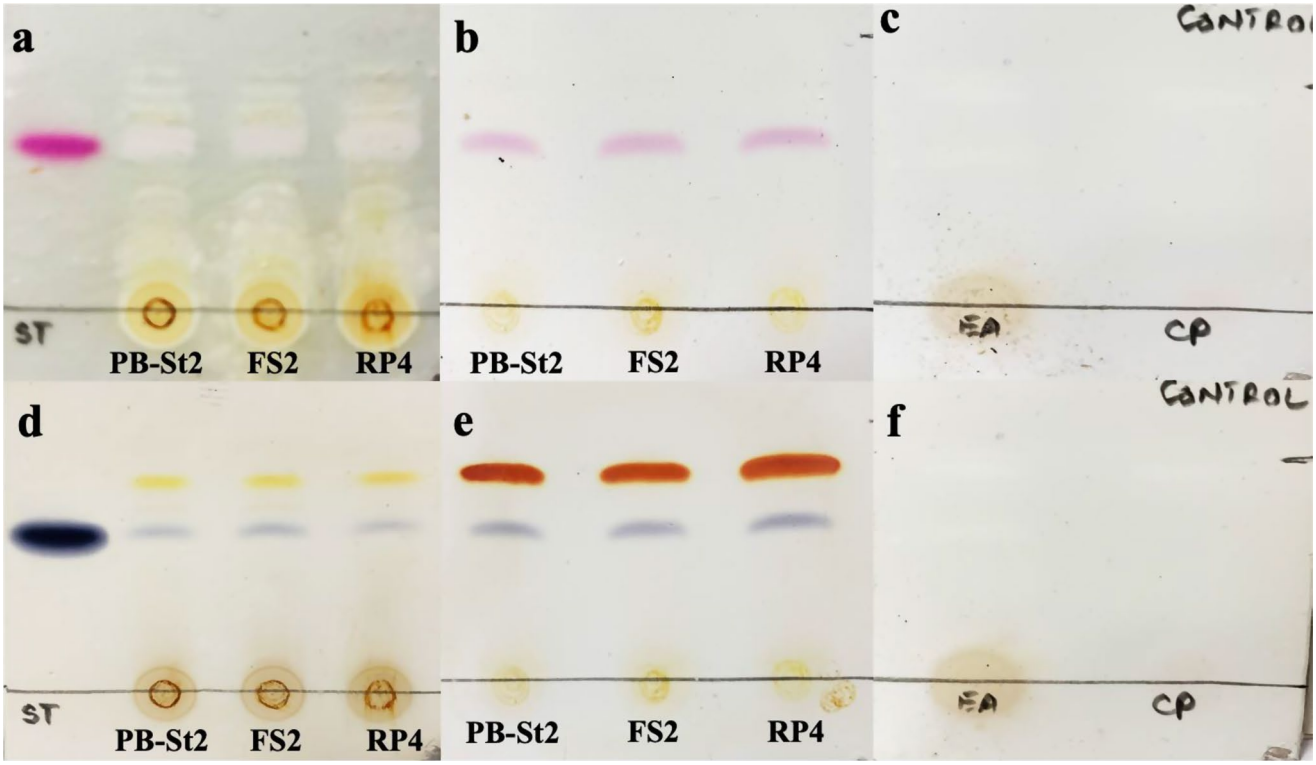

Fig. 1 Pyrrolnitrin (PRN) detection through TLC in the wild type *Pseudomonas* strains. Fresh TLC after spraying; Identification of Pyrrolnitrin production in the (**a**) supernatant and (**b**) cell pellet of wild type *Pseudomonas* strains. (**c**) medium control. 24 h old TLC indicating color change of pyrrolnitrin from pink to purple; (**d**) supernatant and (**e**) cell pellet of wild type *Pseudomonas* strains. (**f**) medium control; EA: Ethyl acetate extraction from supernatant, CP: Acetone extraction from cell pellet

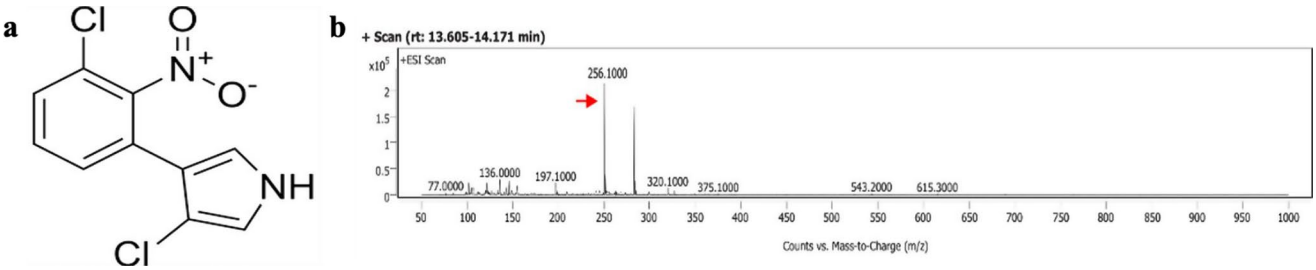

Fig. 2 Identification of pyrrolnitrin (PRN). (**a**) Chemical structure of pyrrolnitrin, (**b**) LC-MS chromatogram representing pyrrolnitrin, m/z $[M+H]^+$ 256.1000

Results

Characterization and purification of Pyrrolnitrin

All three *Pseudomonas* strains exhibited pyrrolnitrin production in supernatant and pellet extracts. This was evidenced by the formation of pink bands on TLC plates immediately after spraying with Ehrlich Reagent (Fig. 1a-c), which later changed to dark blue after 24 h (Fig. 1d-f). The compound was purified using HPLC, identified through LC-MS library and compared with standard reference data of pyrrolnitrin previously identified from PB-St2. The chromatograms verified pyrrolnitrin with m/z $[M+H]^+$ 256.1 (Fig. 2).

Antimicrobial analysis of purified Pyrrolnitrin

The antifungal activities of purified pyrrolnitrin, at a concentration of 100 µg, against plant pathogens demonstrated strong efficacy against *Alternaria* sp., evidenced by a 4.5 cm inhibition zone followed by *Fusarium* sp., *Colletotrichum* sp., and *Aspergillus* sp. (Fig. 3a). Notably, pyrrolnitrin significantly impeded spore formation in the tested fungal strains. Hemocytometer analysis indicated that spore production decreased by 82% in *Alternaria* sp., 75% in *Aspergillus* sp., 56.5% in *Fusarium* sp., and 61% in *Colletotrichum* sp. (Fig. 3b). Fluorescence microscopy examination revealed a reduction in spore count compared to the

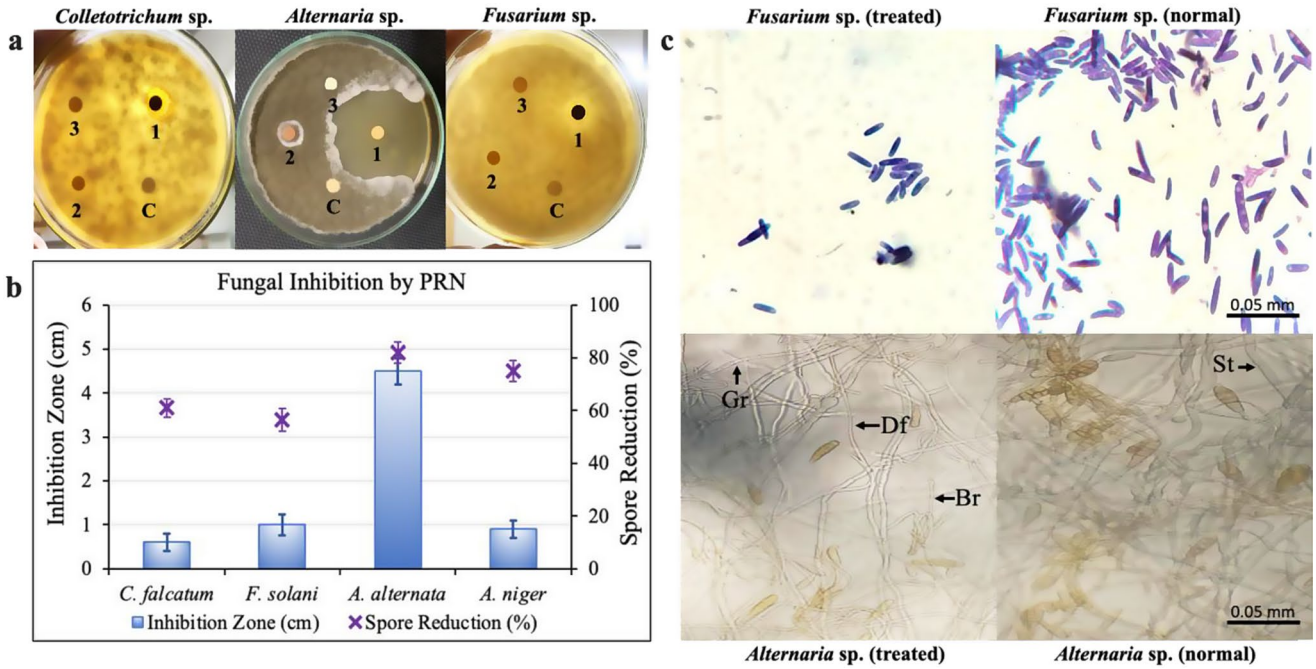

Fig. 3 Antifungal potential of pyrrolnitrin (PRN). (**a**) Antifungal plate assay of pyrrolnitrin against (**1**) *Colletotrichum* sp., (**2**) *Alternaria* sp. and (**3**) *Fusarium* sp. 1 = pyrrolnitrin, 2 = extract of PB-St2, 3 = control (extract of BL21 with trp), C = control (methanol). (**b**) Graphical representation measuring zone of inhibition and spore reduction by pyrrolnitrin against selected fungal phytopathogens. (**c**) Fluorescent microscopy (254 nm, 40X) observations revealing the effect of pyrrolnitrin on (**1**) *Fusarium* sp. with reduction in spore formation (**2**) normal production of spores, (**3**) *Alternaria* sp. with reduced spore formation, granulations in hyphae and increased branching compared to the (**4**) untreated *Alternaria* sp. with septate in hyphae and high sporulation. Df: Deformation, Gr: Granulations, Br: Branching, St: Septate

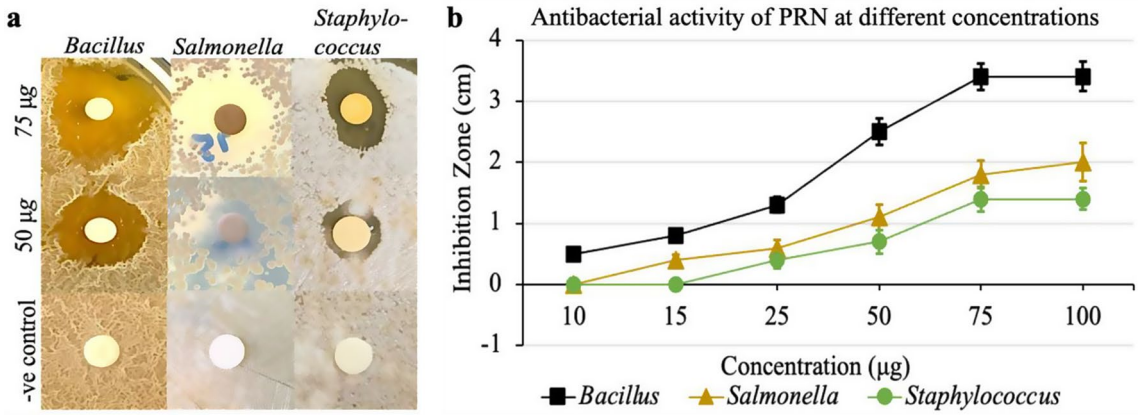

Fig. 4 Antibacterial potential of pyrrolnitrin (PRN). (**a**) Antagonistic plate assay of pyrrolnitrin against *Bacillus cereus*, *Salmonella enterica* and *Staphylococcus* sp. (**b**) Graph depicting antibacterial activity of pyrrolnitrin, at different concentrations, against the selected bacterial pathogens

control, as well as substantial hyphal deformations in *Alternaria* sp. and *Fusarium* sp. (Fig. 3c).

Purified pyrrolnitrin from *Pseudomonas* strains PB-St2, FS2, and RP4 also showed antibacterial activity against *Bacillus* sp. with an inhibition zone of 2.5 cm (at 50 µg concentration of pyrrolnitrin), 3.4 cm (at 75 µg concentration of pyrrolnitrin), and *Salmonella* sp. with an inhibition zone of 1.8–2 cm at 75–100 µg pyrrolnitrin concentration. Antibacterial activity of pyrrolnitrin against *Staphylococcus* sp. was observed with an inhibition zone of approximately 1.4 cm only at 75 µg pyrrolnitrin concentrations (Fig. 4). No activity was observed against *Pseudomonas aeruginosa*, and *Klebsiella* sp.

Anticancer activity of Pyrrolnitrin

Pyrrolnitrin´s cytotoxic effects were evaluated on HepG-2 and SF767 cancer cell lines using various concentrations. The experiments, conducted using microtiter plates, included PB-St2, FS2, and RP4 extracts as a positive control

and methanol as a negative control for both cell lines. In the HepG-2 cell line, pyrrolnitrin exhibited an IC_{50} at 15 µg, with complete cell death observed at 75 µg. For the SF767 cell line, the IC_{50} of pyrrolnitrin was reached at 25 µg. When treated with 100 µg of pyrrolnitrin, only 5% of SF767 cells remained viable (Fig. 5).

Fungicidal activity of heterologous Pyrrolnitrin clones against *Alternaria* Sp

Successful cloning of the complete sequence was confirmed by digesting the constructs with *Eco*RI and *Bam*HI restriction enzymes (Fig. S2). Restriction digestion of the empty plasmid generated a single band of approximately 3 kb (exact 2961 bp) on the gel with *Eco*RI.

The purified pyrrolnitrin from wild type *Pseudomonas* strains exhibited the maximum effectiveness against the *Alternaria* sp. (Fig. 3), prompting the evaluation of heterologous clones against two distinct *Alternaria* sp. strains. A plate assay demonstrated that the PBP1 clone (of strain PB-St2) displayed the most potent inhibitory effect, with 57% and 70% inhibition against two *Alternaria* strains tested, respectively. The clone FBP2 (of strain FS2) showed inhibition rates of 51.1% and 61.34%, while RBP3 (of strain RP4) exhibited 55.88% and 68.21% inhibition against *Alternaria* 1 and *Alternaria* 2 strains, respectively. Additionally, the PBP1 clone was the most effective in suppressing spore production, achieving approximately 77% and 82% inhibition for *Alternaria* 1 and *Alternaria* 2 strains, followed by FBP2 with 61% and 70% inhibition. The clone RBP3 demonstrated 56% and 54% inhibitory activity against spore production (Fig. 7, Fig. S5).

Pyrrolnitrin knockdown mutants showed decreased antifungal potential

The knockdown constructs were verified by restriction digestion and PCR amplification. The empty vector, pKC1132 when digested with *Xba*I generated a single band of 3443 bp and the construct pKCPN generated a single band

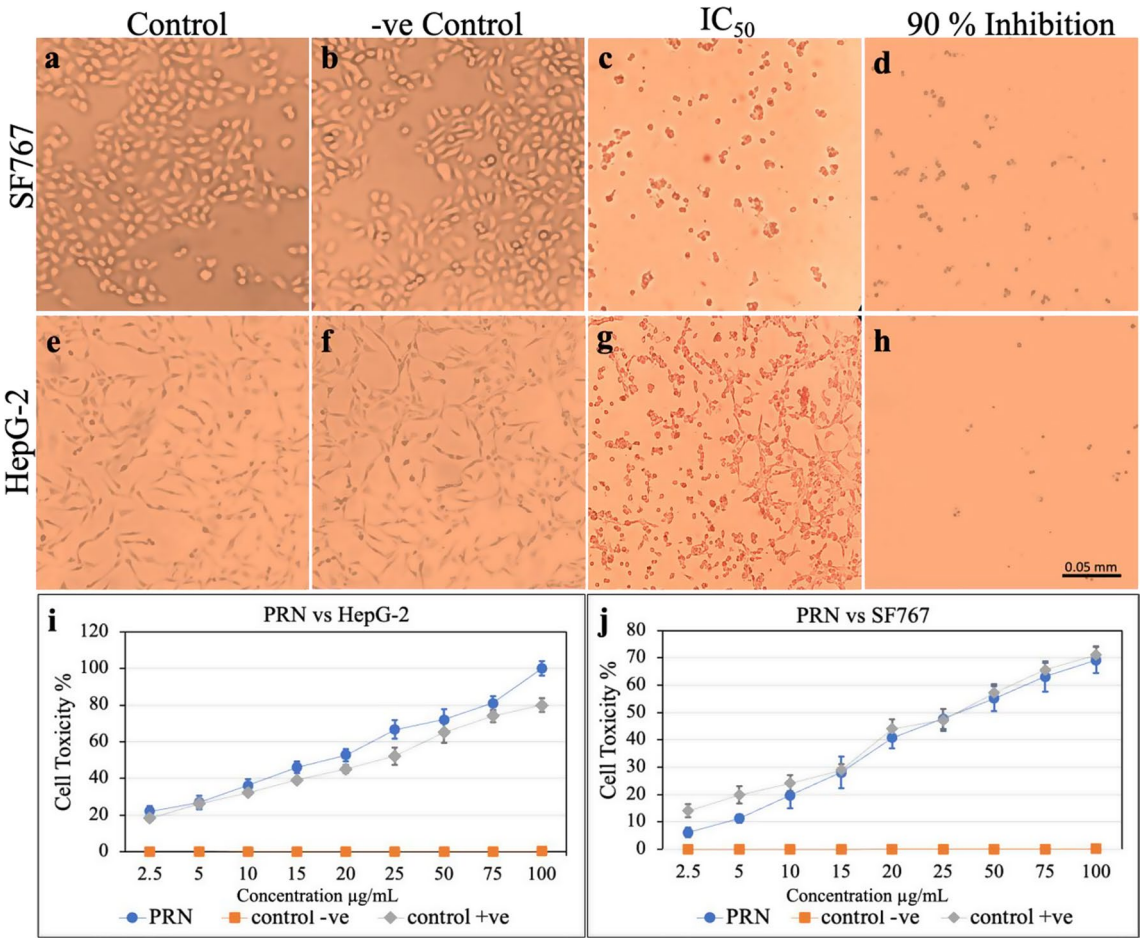

Fig. 5 Anticancer activity of pyrrolnitrin (PRN). Light microscopy (40X) observation revealing the effect of pyrrolnitrin against (**a**-**d**) HepG-2 and (**e**-**h**) SF767 cell lines. Control and negative control depict the morphology of healthy cells. Graphical representation of MIC of pyrrolnitrin against (**i**) HepG-2 cancer cell line and (**j**) SF767 cancer cell line

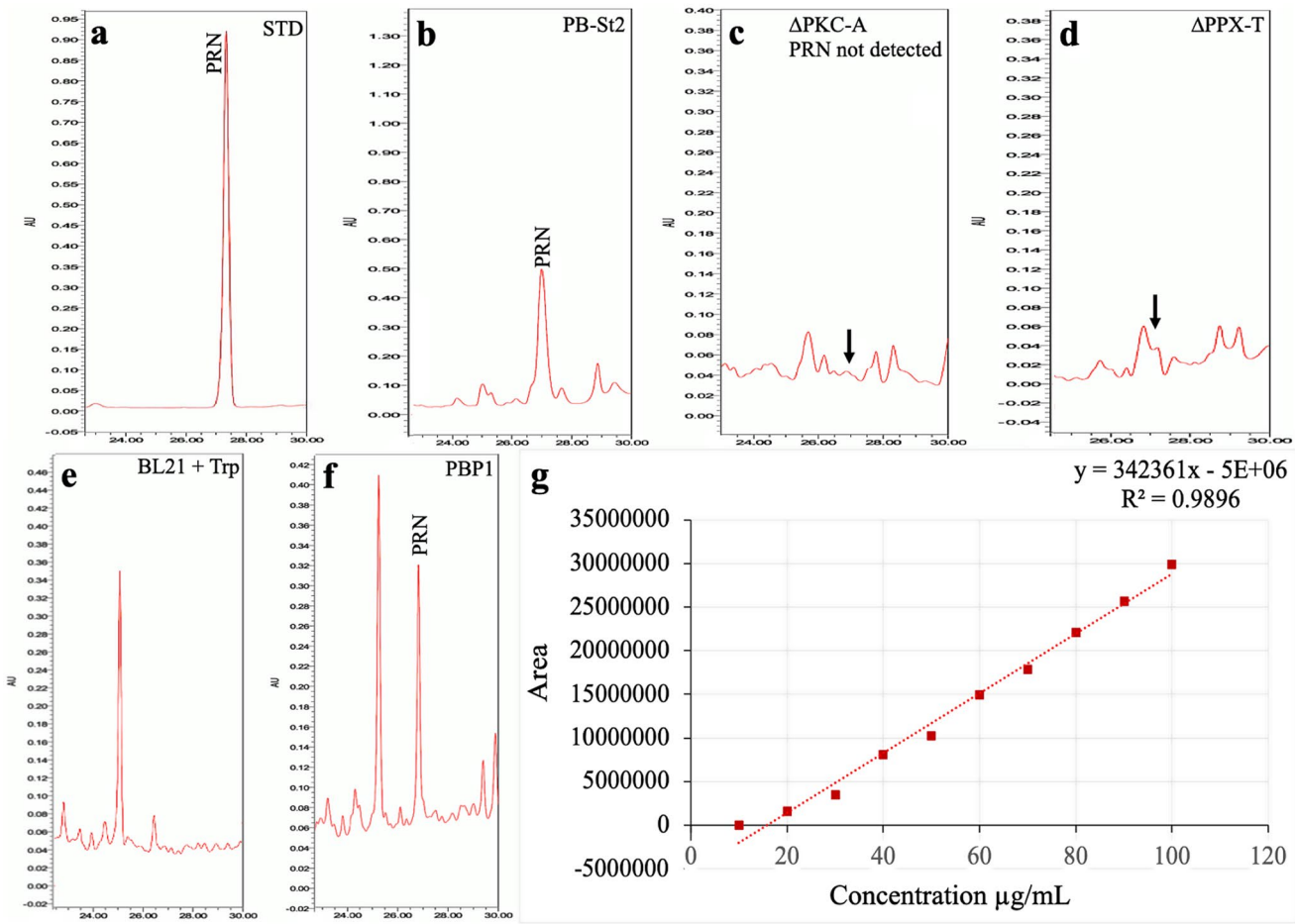

Fig. 6 Quantification of pyrrolnitrin (PRN). HPLC chromatograms representing (**a**) standard of pyrrolnitrin (PRN), (**b**) standard of phenazine-carboxylic acid (PCA), (**c**) standard of tryptophan (TRP), (**d**) wild type crude extract of PB-St2 as positive control showing peaks for phenazine-1-carboxylic acid and pyrrolnitrin, (**e**) crude extract of PB-St2 mutant derived by pKCPN revealing reduced phenazine-1-carboxylic acid production and absence of pyrrolnitrin peak, (**f**) crude extract of PB-St2 mutant derived by pEXPN revealing reduction in phenazine-1-carboxylic acid and pyrrolnitrin peaks, (**g**) crude extract of BL21 strain as negative control, (**h**) crude extract of BL21 induced with tryptophan as negative control showing a peak of only TRP, (**i**) crude extract of PBP1 showing production of pyrrolnitrin when induced with tryptophan. (**j**) Graph showing standard curve of pyrrolnitrin. Blue arrow: peak of pyrrolnitrin, red arrow: peak of PCA, green arrow: peak of tryptophan

of 3972 bp. In contrast, double digestion of the construct pKCPN with *Eco*RV + *Xba*I generated two bands of 3417 bp and 555 bp and *Xho*I bands of 2020 bp and 1952 bp, respectively. Moreover, the empty vector pEX18Tc generated two bands of 3955 bp and 2394 bp construct pEXPN and two bands of 3955 bp and 2936 bp. The pEX18Tc showed a single band of 6349 bp after digestion with *Eco*RV. The construct pEXPN showed three bands after digestion with *Ksp*AI and *Xho*I with sizes of 3206, 2863, and 822 bp. Moreover, PCR amplification of the knockdown constructs confirmed ligation of the 540 bp insert (Fig. S2). Extracts from pyrrolnitrin-deficient mutants showed no bands and peaks corresponding to pyrrolnitrin when subjected to TLC and HPLC analyses. Wild type strains exhibited pyrrolnitrin production of approximately 34–44 µg/mL, as revealed by HPLC analysis of their extracts. In contrast, pyrrolnitrin was not detectable in extracts from pKCPN-derived mutants, verifying the suppression of pyrrolnitrin synthesis. Strains transformed with pEXPN, however, demonstrated minimal pyrrolnitrin production, ranging from 8 to 10 µg/mL (Fig. 6; Table 4, Fig. S4, S6).

Pyrrolnitrin-deficient mutants of *Pseudomonas* strains PB-St2, RP4 and FS2 exhibited reduced fungicidal activities against all tested fungal pathogens, advocating the contribution of pyrrolnitrin in antifungal potential of *P. aurantiaca* strains. Plate assays indicated that relative to the wild type *Pseudomonas* strain, the antifungal activity of ΔPKC-A mutant of PB-St2 against *Alternaria* sp. was diminished by 45%, while the ΔPPX-T mutant exhibited a reduction of 21.21% in its antifungal potential. Similar trends were observed with *Aspergillus* sp., where ΔPKC-A showed a 52% decrease in antifungal efficacy followed

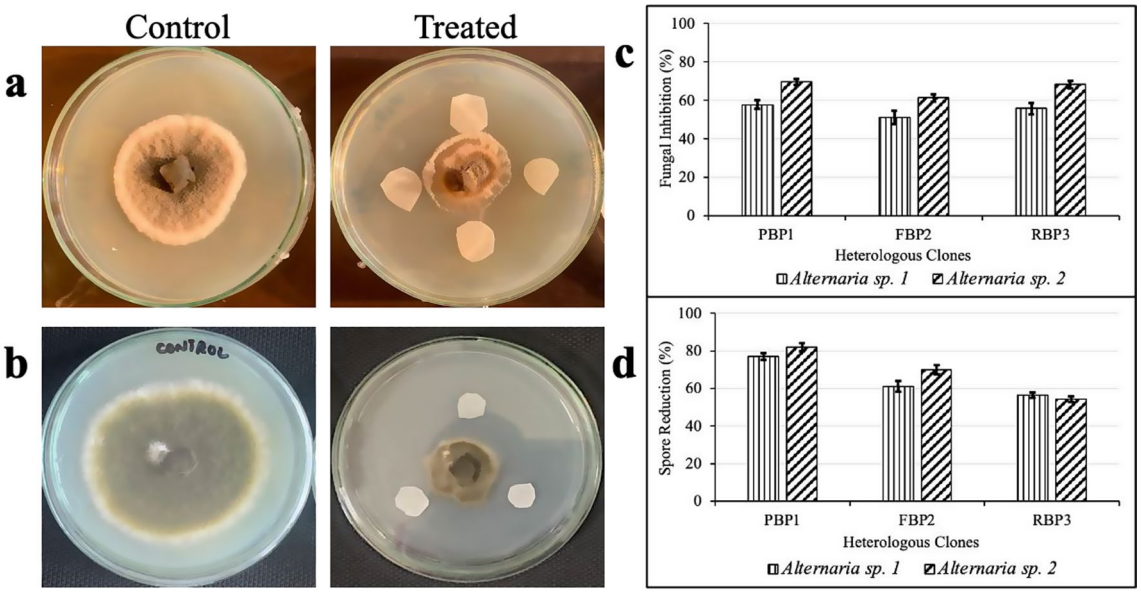

Fig. 7 Antifungal analysis of heterologous clones. (**a**, **b**) Plate assay of heterologous clones against two Alternaria strains, (**c**, **d**) Fungal spore reduction counted by hemocytometer

Table 4 Quantification of Pyrrolnitrin and phenazine-1-carboxylic acid (PCA) in Pyrrolnitrin knockdown mutants

Metabolites (µg/mL)	PB-St2	ΔPKC-A	ΔPPX-T	PBP1 + Trp
Pyrrolnitrin	36 ± 2.05	ND	9.77 ± 0.67	21 ± 1.22
PCA	228.03 ± 5.73	57.17 ± 6.13	88.25 ± 5.17	ND
	FS2	**ΔFKC-A**	**ΔFPX-T**	**FBP2 + Trp**
Pyrrolnitrin	34 ± 1.11	ND	8.13 ± 1.55	18.44 ± 2.01
PCA	317.31 ± 6.22	84.22 ± 3.74	166.18 ± 12.22	ND
	RP4	**ΔRKC-A**	**ΔRPX-T**	**RBP3 + Trp**
Pyrrolnitrin	44 ± 2.05	ND	9.87 ± 1.17	19.02 ± 1.19
PCA	322.09 ± 8.41	92.27 ± 7.03	221.74 ± 4.17	ND

Results are displayed as average of triplicates

by ΔPPX-T that showed a 30% reduction. For *Fusarium* sp., the antifungal potential of the mutants ΔPKC-A and ΔPPX-T decreased by 28.9% and 21.05%, respectively. Likewise, ΔPKC-A showed 31.7% decrease in its antifungal potential against *Colletotrichum* sp., while ΔPPX-T showed only 26.8% decrease (Figs. 8 and 9).

The fungicidal potential of ΔFKC-A (knockdown mutant of FS2) against *Alternaria* sp. was reduced by 31.7% and of ΔFPX-T by 14.6%. Similar results were observed for *Aspergillus* sp., where ΔFKC-A showed a decrease of 36% in its inhibitory activity. Nevertheless, no significant variation in antifungal potential against *Fusarium* sp. was witnessed by pyrrolnitrin deficient mutants in comparison to wild type FS2. The mutant ΔFKC-A of strain FS2 showed 76% decrease in its antifungal potential against *Colletotrichum* sp. The significant loss of fungicidal potential was observed by ΔRKC-A (pyrrolnitrin knockdown mutant of strain RP4) with 27.5%, 22.5%, 26.3% and 42.2% against *Colletotrichum* sp., *Fusarium* sp., *Alternaria* sp., and *Aspergillus* sp., respectively (Figs. 8 and 9).

Spore counts obtained using hemocytometer indicated that PKCPN derived mutants lost their ability to inhibit spore production in fungi when compared to the wild-type strains. Results demonstrated that pyrrolnitrin-deficient mutants of PB-St2 exhibited a significant reduction in their ability to suppress spore production: 82.88% for *Alternaria* sp., 73.12% for *Aspergillus* sp., 67.16% for *Colletotrichum* sp., and 66.6% for *Fusarium* sp. Similarly, the mutant ΔFKC-A also showed significantly decreased spore inhibition relative to the wild type FS2 strain, losing 23.7% efficacy against *Fusarium* sp., 58.1% against *Alternaria* sp., 64.25% against *Aspergillus* sp., and 69.5% against *Colletotrichum* sp. Likewise, compared to the wild type RP4, mutant ΔRKC-A lost 40.7% spore inhibition potential against *Fusarium* sp., 47.9% against *Alternaria* sp., 43.5% for *Aspergillus* sp. and 47.5% for *Colletotrichum* sp. (Fig. 10).

When observed under a stereomicroscope, antifungal plates revealed a clear inhibition zone around the wild-type PB-St2 strain with no hyphal or spore production. In contrast, plates co-cultured with mutant strains showed fused mycelial growth and spores around the bacterial inoculum (Fig. 10).

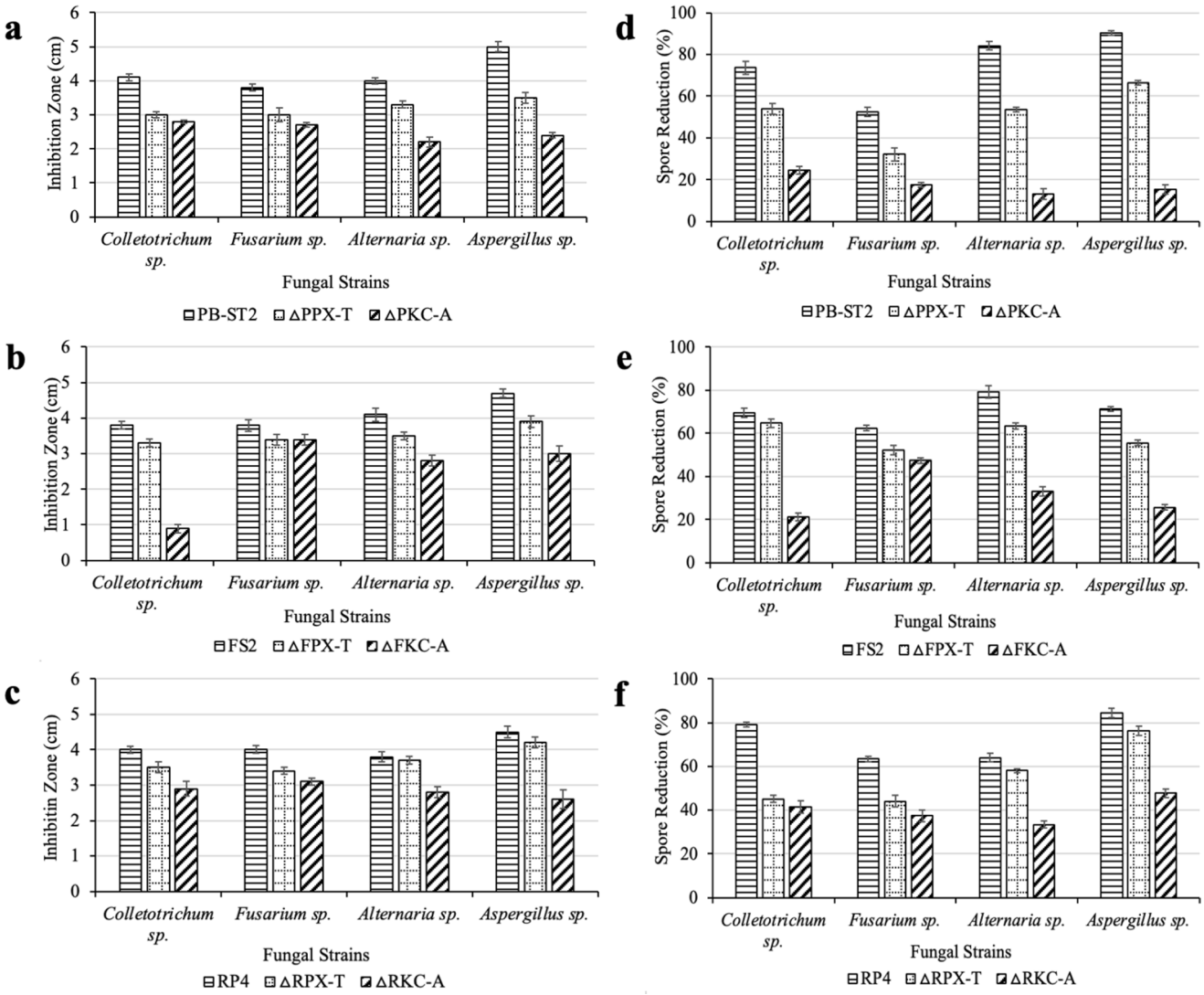

Fig. 8 Analysis of antifungal activity in mutants. (**a-c**) Graphs representing the inhibition zones measured from antifungal plates of wild type and mutant *Pseudomonas* strains, (**d-f**) Graphs representing average percent reduction in spore inhibition of fungal strains by both wild type and mutant strains. The error bars represent standard deviation where results are means of three replicates

Pyrrolnitrin knockdown mutants showed decreased phenazine biosynthesis and impacted growth kinetics

Unexpectedly, all knockdown mutants of *Pseudomonas* strains PB-St2, FS2, and RP4 displayed alterations in morphology when compared to their wild-type counterparts. The distinctive orange coloration, indicative of phenazine production in *P. chlororaphis* strains, shifted to yellow in the knockdowns (Table 4; Fig. 11).

Furthermore, these mutants exhibited slow growth during cultivation. Such as, after 24 h, the wild-type strains PB-St2, FS2, and RP4 reached optical densities of 1.32, 1.25, and 1.22, respectively. In contrast, the mutants ΔPKC-A, ΔFKC-A, and ΔRKC-A achieved optical densities of 0.72, 0.85, and 0.77. Similarly, ΔPPX-T, ΔFPX-T, and ΔRPX-T mutants showed optical densities of 0.88, 0.92, and 0.88. Computational analysis of the pyrrolnitrin biosynthetic gene cluster revealed sequence homology between the tryptophan halogenase (*prn*A) nucleotide sequence and thioredoxin reductase (*trx*R). The *trx*R gene is a component of the thioredoxin system (TS), which plays a role in NADPH reduction, crucial for catalytic reactions in major secondary metabolite pathways. Additionally, *trx*R is involved in DNA replication, explaining that its reduced expression impacts cellular replication and growth (Fig. S7).

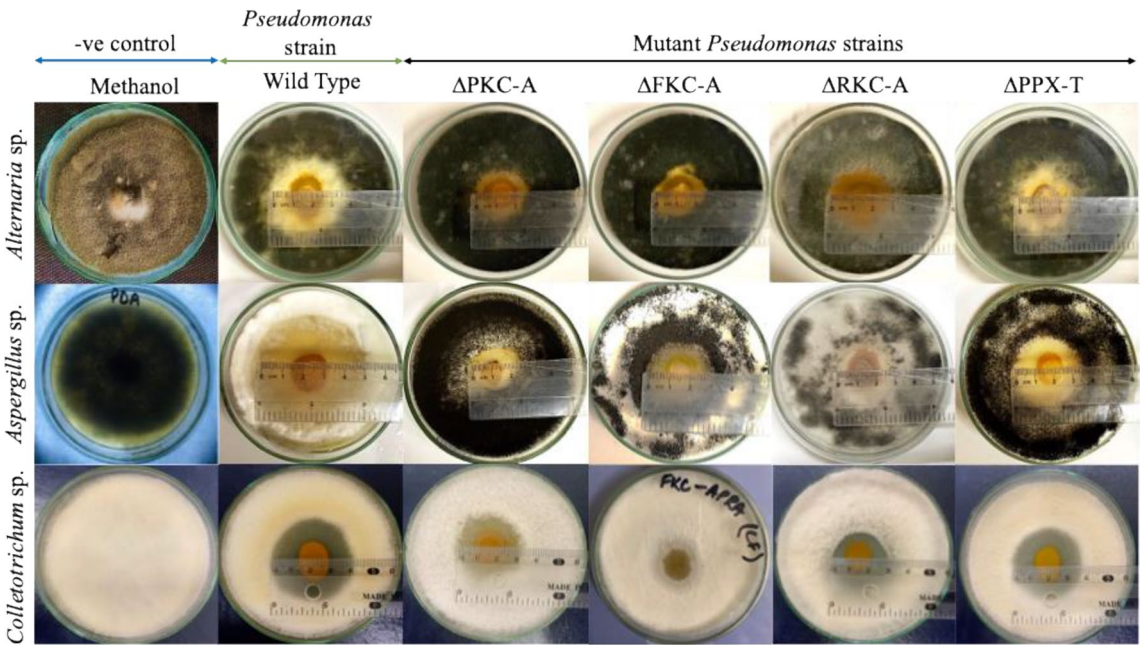

Fig. 9 Antifungal activity of wild type and mutant *Pseudomonas* sp. strains against fungal pathogens. Antifungal plate assays; comparison of antagonistic activity of wild type *Pseudomonas* strain with developed mutant strains, against *Alternaria* sp., *Aspergillus* sp., and *Colletotrichum* sp. pKCPN derived mutants (ΔPKC-A, ΔFKC-A, ΔRKC-A) showing reduced antifungal activity compared to pEXPN derived mutant (ΔPPX-T)

Discussion

The biological control of plant pathogens involves various bacterial genera like *Burkholderia*, *Serratia*, *Pseudomonas*, and *Bacillus*. *Pseudomonas* spp. is notable for their widespread presence and production of phenazines, broad-spectrum antifungal compounds. *Pseudomonas* also synthesizes metabolites that enhance antifungal capabilities and aid survival under biotic stress (Höfte 2021; Navarro-Monserrat and Taylor 2023; Vasanthabharathi and Jayalakshmi 2018). The *P. chlororaphis* group is significant due to its potential as bio-stimulants and bio-fungicides in crops, producing volatile organic compounds, siderophores, and phytohormones, benefiting plants (Raj et al. 2020). *P. chlororaphis* subsp. *aurantiaca* strains FS2 and PB-St2, and *P. chlororaphis* subsp. *chlororaphis* RP4 are documented for plant growth promotion and synthesis of diverse secondary metabolites, with primary focus on antifungal activity attributed to phenazines (Fakruddin et al. 2022; Shishir and Hoq 2020; Shahid et al. 2021).

This study specifically elucidated the function and significance of pyrrolnitrin in these strains examining their antagonistic properties against various fungal plant pathogens. The purified pyrrolnitrin extracted from all three strains demonstrated effective inhibition against all tested fungal pathogens, resulting in a reduction of up to 82% in spore formation among them. Antifungal potential of pyrrolnitrin is a well-documented phenomenon and has been shown in several studies (Jug et al. 2018; Mohamed et al. 2020; Zhang et al. 2020a, b, c, d). In addition to antifungal activities, pyrrolnitrin isolated from strains PB-St2, FS2, and RP4 showed antibacterial properties against *Bacillus* sp., *Salmonella* sp., and *Staphylococcus* sp. strains. These findings are consistent with previously reported antibacterial effects of pyrrolnitrin against *Agrobacterium tumefaciens*, *Corynebacterium insidiousum*, *P. syringae*, and *Xanthomonas campestris*, with MIC of 1 µg /mL. Bacterial pathogens *Clavibacterium michiganense* and *S. marcescens*, were inhibited at MIC levels of 10 µg/mL or greater (Cherin et al. 1996). Nonetheless, no substantial reports were identified that could indicate pyrrolnitrin's antibacterial properties. Additionally, purified pyrrolnitrin also showed antiproliferative potential against HepG-2 and SF767 cancer cell lines. In the HepG-2 cell line, pyrrolnitrin exhibited an IC_{50} at 15 µg, with complete cell death observed at 75 µg, whereas, for the SF767 cell line, the IC_{50} of pyrrolnitrin was reached at 25 µg. Previous studies have shown the antiproliferative activity of several of pyrrole derivatives indicating their therapeutic potential, however, purified pyrrolnitrin has been reported a little for anticancer potential (Ahmad et al. 2018).

Owing to its broad-spectrum biological activities, the entire *prn*ABCD operon, spanning 6.1 kb, along with its promoter region, was transformed into *E. coli* to optimize the heterologous expression. This approach sought to determine whether pyrrolnitrin production was dependent on additional factors or genes, or if the upstream promoter region alone

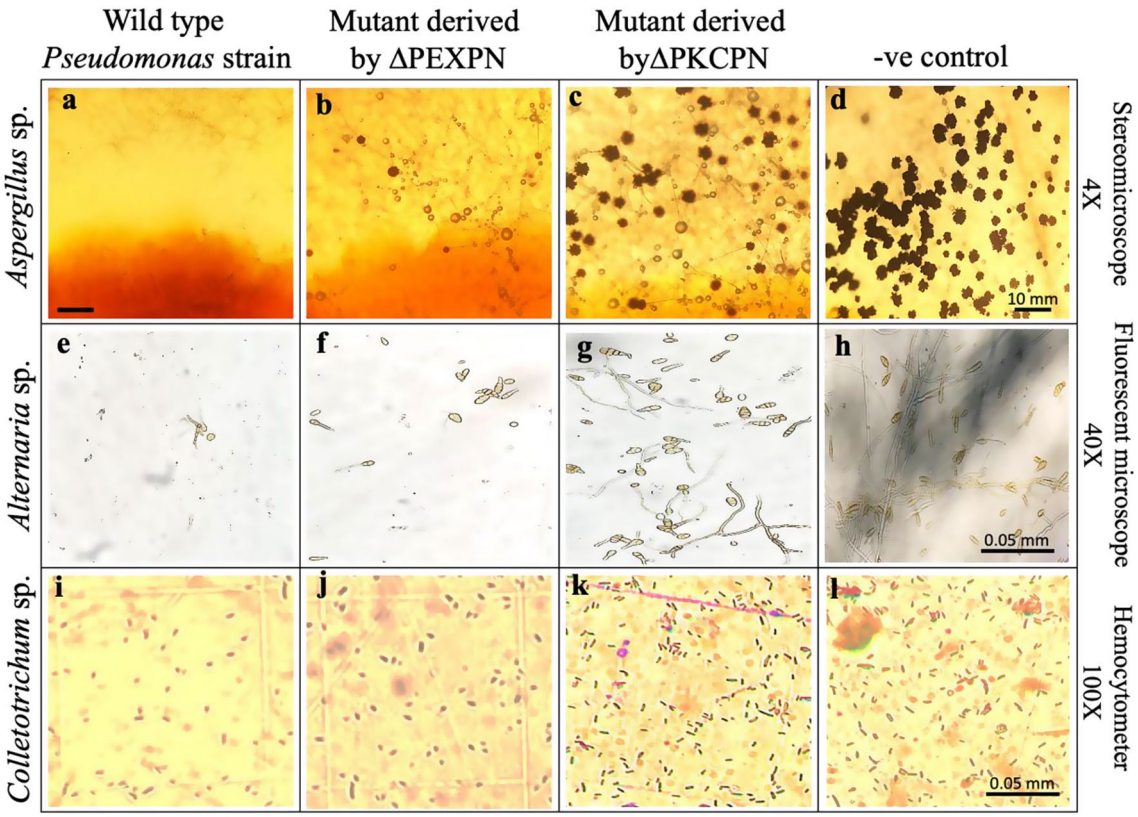

Fig. 10 Microscopic comparisons of antifungal activity in wild-type and mutant *Pseudomonas* strains against fungal pathogens. (**a**-**d**) Stereomicroscopy (40X) observations against *Aspergillus niger* revealing reduced inhibition activity by mutants; (**a**) clear zone of inhibition can be observed between wild type and hyphae of *Aspergillus* with no spore production, (**b**) No inhibition zone can be observed after treatment with ΔPPX-T with few spores production, (**c**) High hyphae proliferation around ΔPKC-A with increase in spore production as well, (**d**) negative control. (**e**-**h**) Fluorescent microscopy (40X) observations against *Alternaria alternata* revealing (**g**) loss of inhibition activity by ΔPKC-A as high number of spores production can be observed. (**i**-**l**) Hemocytometer observations against *Fusarium* sp. (**k**) revealing reduced inhibition activity by ΔPKC-A as high production of spores can be observed

was sufficient for expression. Heterologous expression of bacterial secondary metabolites and biosynthetic gene clusters is a powerful tool for natural product discovery, production optimization, and biosynthetic pathway elucidation (Frias et al. 2018; He et al. 2018). It facilitates the transfer of biosynthetic pathways from slow-growing or genetically intractable organisms to more amenable host systems, thereby improving production efficiency and genetic manipulation capabilities (Hao et al. 2019; Sharma et al. 2020). This approach also allows for the expression of large and complex biosynthetic gene clusters, such as those encoding polyketide synthases (PKS) and non-ribosomal peptide synthetases (NRPS), in well-characterized host organisms (Sharma et al. 2020). The T7 promoter in the pBluescript plasmid facilitates heterologous expression, offering the advantages of robust expression levels and the potential for the heterologous product to constitute up to 50% of the total cellular protein content (Kielkopf et al. 2021).

The antifungal activity and biological control potential of pyrrolnitrin remained unchanged when expressed heterologously in *E. coli*. These engineered bacteria offer an efficient alternative to the lengthy process of cultivating *Pseudomonas* strains and extracting pyrrolnitrin. These engineered clones can be utilized for pyrrolnitrin production and incorporated into fungicidal formulations for inhibition of specific pathogens and can be further enhanced for large-scale pyrrolnitrin synthesis. Some of the previous studies have demonstrated the benefits of expressing pyrrolnitrin operon in heterologous systems. For instance, the entire *prn*ABCD operon from *P. protegens* Pf-5 was successfully expressed in tomato plants utilizing the plant universal vector IL-60. It resulted in the manifestation of a distinct plant phenotype exhibiting resistance to damping-off disease caused by *R. solani* (Mozes-Koch et al. 2012). In silico analysis of PB-St2 genome verified the intactness of entire pyrrolnitrin operon and only a single copy of *prn*ABCD loci was located in the genome. The four genes responsible for pyrrolnitrin production were present on two open reading frames (ORFs), where *prn*A, *prn*C and *prn*D were on frame 1, whereas, *prn*B on frame 2.

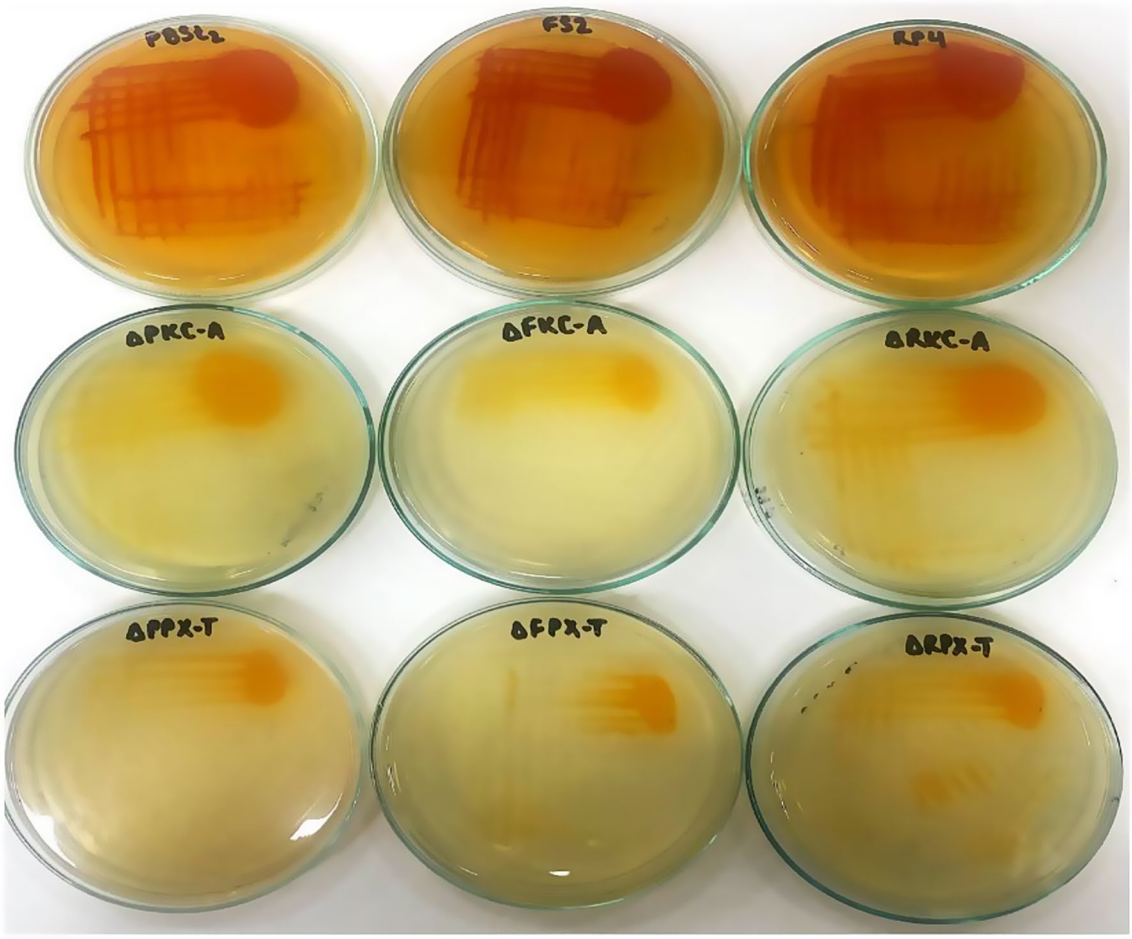

Fig. 11 Morphological pigment variation in the pyrrolnitrin-deficient mutant strains compared to the wild type *P. chlororaphis* strains

As previously mentioned, *P. chlororaphis* strains PB-St2, FS2, and RP4 have been thoroughly demonstrated to possess phenazines-based antifungal activities. To determine whether pyrrolnitrin also contributes to the antifungal capabilities of these strains, knockdown mutants which suppressed the production of pyrrolnitrin, were generated, resulting in reduced antifungal activities. Part of *prn*A gene encoding tryptophan halogenase was targeted to suppress its expression of pyrrolnitrin operon. The approach used in this study specifically used antisense DNA, as they are fairly stable compared to RNAs, and the length was enhanced to avoid nonspecific silencing. Analysis of the mutants with reduced gene expression, created using the pEXPN construct, showed a decrease in pyrrolnitrin levels when subjected to TLC and HPLC validation. Pyrrolnitrin knockdowns exhibited a reduction in fungicidal effectiveness of up to 51% and were incapable of inhibiting spore production. They displayed a significant decrease of 82% in their ability to suppress spores and demonstrated diminished efficacy in restricting mycelial growth when compared to wild-type strains. This finding highlights the crucial role of pyrrolnitrin in shaping the antifungal characteristics of *P. chlororaphis* strains PB-St2, FS2, and RP4.

Unexpectedly, the removal of the *prn*A gene in pyrrolnitrin knockdowns not only impacted the antifungal capabilities but also changed the phenazine biosynthesis. The elimination of *prn*A resulted in decreased synthesis of the characteristic orange pigment (phenazine-1-carboxylic acid) and exhibited slower growth rates compared to wild-type strains. Analysis using high-performance liquid chromatography (HPLC) showed reduced PCA biosynthesis in pyrrolnitrin knockdowns. Additionally, the cell density of the mutant strains after 24 h of cultivation was half that of the wild-type strains. Subsequent computational analysis showed homology of *prn*A with thioredoxin reductase (*trx*R) gene. Thioredoxin reductase (*trx*R) is crucial in DNA replication, bacterial metabolism, NADPH reduction, and maintenance of redox balance of the cell, and is regulated by the thioredoxin system (TS) which includes two antioxidant oxidoreductases, Trx and *trx*R, with NADPH as an electron donor and regulates ribonucleotide activity (Karlenius and Tonissen 2010). The diverse roles and importance of

the *trx*R gene underscore its crucial role in sustaining cellular growth dynamics, while its elimination confirms the slower growth rates and decreased phenazine biosynthesis as observed in pyrrolnitrin knockdowns. While the precise molecular process through which the removal of the *prn*A gene affected phenazine production requires further investigation, it confirms that *prn*A is crucial in sustaining the biological control capabilities of *P. chlororaphis* strains PB-St2, FS2, and RP4.

In conclusion, the study highlights the pivotal role of pyrrolnitrin in the antifungal activity of *Pseudomonas chlororaphis* strains PB-St2, FS2, and RP4. Purified pyrrolnitrin effectively inhibited multiple mycopathogens, suppressing spore formation by up to 82%. Beyond its antifungal action, it also demonstrated antibacterial effects and antiproliferative activity against cancer cell lines. The complete *prn*-ABCD operon was successfully heterologously expressed in *E. coli*, preserving its antifungal efficacy and supporting its potential use in fungicidal formulations. Interestingly, pyrrolnitrin knockdown mutants not only showed diminished antifungal performance but also disrupted phenazine biosynthesis and exhibited slower growth. Computational analysis revealed homology between *prn*A and thioredoxin reductase (*trx*R), a key enzyme in bacterial metabolism, DNA replication, and redox regulation. Collectively, these findings underscore pyrrolnitrin's central role in the biocontrol potential of *P. chlororaphis* and its broader regulatory influence on secondary metabolite pathways.

Supplementary Information The online version contains supplementary material available at https://doi.org/10.1007/s11274-025-04413-8.

Acknowledgements Authors would like to acknowledge Prof. Dr. Harald Gross (University of Tuebingen, Department of Pharmaceutical Biology), Alexander Von Humbolt (AvH) Foundation, Bonn-Bad Godesberg (Federal Republic of Germany) for providing equipment grant to Dr. Samina Mehnaz.

Author contributions Conceptualization: [Mahnoor Zameer, Samina Mehnaz, Deeba Noreen Baig]; Data curation: [Mahnoor Zameer, Samina Mehnaz, Andreas Bechthold]; Formal analysis: [Mahnoor Zameer, Samina Mehnaz]; Investigation: [Mahnoor Zameer]; Methodology: [Samina Mehnaz, Andreas Bechthold, Deeba Noreen Baig]; Project administration: [Mahnoor Zameer, Samina Mehnaz, Andreas Bechthold]; Resources: [Samina Mehnaz, Roman Makitrynskyy, Andreas Bechthold, Kauser Abdulla Malik]; Supervision: [Samina Mehnaz, Deeba Noreen Baig]; Validation: [Mahnoor Zameer, Samina Mehnaz, Izzah Shahid, Andreas Bechthold]; Visualization: [Mahnoor Zameer, Samina Mehnaz]; writing-original draft: [Mahnoor Zameer, Samina Mehnaz]; writing-review and editing: [Mahnoor Zameer, Izzah Shahid, Andreas Bechthold, Samina Mehnaz]. I certify that the above information is true and correct. All the authors contributed to the study and the manuscript. If the manuscript is accepted for publication, I agree to transfer all copyright ownership of the manuscript to the World Journal of Microbiology and Biotechnology, which covers the rights to use, reproduce, or distribute the article.

Funding Mahnoor Zameer was supported by a PhD fellowship by Higher Education Commission (HEC) of Pakistan.

Data availability Data is provided within the manuscript.

Declarations

Competing interests The authors declare no competing interests.

References

Abd El-Hameed RH, Sayed AI, Mahmoud Ali S, Mosa MA, Khoder ZM, Fatahala SS (2021) Synthesis of novel pyrroles and fused pyrroles as antifungal and antibacterial agents. J Enzyme Inhib Med Chem 36(1):2183–2198

Ahmad S, Alam O, Naim MJ, Shaquiquzzaman M, Alam MM, Iqbal M (2018) Pyrrole: an insight into recent Pharmacological advances with structure activity relationship. Eur J Med Chem 5(157):527–561

Bajpai A, Singh B, Joshi S, Johri BN (2018) Production and characterization of an antifungal compound from Pseudomonas protegens strain W45. Proc Natl Acad Sci India Sect B: Biol Sci 88:1081–1089

Bertani G (1952) Studies on lysogenesis. I. The mode of phage liberation by lysogenic *Escherichia coli*. J Bacteriol 62:293–300

Chen L, Wang Y, Miao J, Wang Q, Liu Z, Xie W, Liu X, Feng Z, Cheng S, Chi X, Ge Y (2021) LysR-type transcriptional regulator FinR is required for phenazine and Pyrrolnitrin biosynthesis in biocontrol *Pseudomonas chlororaphis* strain G05. Appl Microbiol Biotechnol 105:7825–7839

Cherin L, Brandis A, Ismailov Z, Chet I (1996) Pyrrolnitrin production by an *Enterobacter agglomerans* strain with broad-spectrum activity toward fungal and bacterial phytopathogens. Curr Microbiol 32:208–212

Costa R, Van Aarle IM, Mendes R, Van Elsas JD (2009). Genomics of pyrrolnitrin biosynthetic loci: evidence for conservation and whole-operon mobility within Gram-negative bacteria. Environmental Microbiology 11(1):159–175.

De Frias UA, Silva-Rocha R, Guazzaroni ME, Pereira GKB (2018) Boosting secondary metabolite production and discovery through the engineering of novel microbial biosensors. Biomed Res Int 2:1–11. https://doi.org/10.1155/2018/7021826

de Souza JT and Raaijmakers JM (2003). Polymorphisms within the prnD and pltC genes from pyrrolnitrin and pyoluteorin-producing Pseudomonas and Burkholderia spp. FEMS Microbiology Ecology 43(1):21–34.

Fakruddin M, Shishir MA, Yousuf Z, Khan SS (2022) Next generation probiotics- the future of biotherapeutics. Microb Bioact 5(1):156–163

Gonzales MF, Brooks T, Pukatzki SU, Provenzano D (2013) Rapid protocol for Preparation of electrocompetent Escherichia coli and Vibrio cholerae. JoVE 80

Hao T, Lou C, Guo Z, Horsman GP, Chen Y, Merritt J, Zhang G, Zhang Z, Wang M, Wang W, Liu L, Li P, Gao S, Xie Z, Zhao X, Zhang Y (2019) An anaerobic bacterium host system for heterologous expression of natural product biosynthetic gene clusters. Nat Commun 10(1). https://doi.org/10.1038/s41467-019-11673-0

He Y, Wang B, Chen W, Cox RJ, He J, Chen F (2018) Recent advances in reconstructing microbial secondary metabolites biosynthesis in *Aspergillus* spp. Biotechnol Adv 36(3):739–783

Hemeg HA, Moussa IM, Ibrahim S, Dawoud TM, Alhaji JH, Mubarak AS, Kabli SA, Alsubki RA, Tawfik AM, Marouf SA (2020)

Antimicrobial effect of different herbal plant extracts against different microbial population. Saudi J Biol Sci 27(12):3221–3227
Höfte M (2021) The use of *Pseudomonas* spp. As bacterial biocontrol agents to control plant diseases. Burleigh Dodds Sci 301–374. https://doi.org/10.19103/as.2021.0093.11
Huang R, Feng Z, Chi X, Sun X, Lu Y, Zhang B, Lu R, Luo W, Wang Y, Miao J, Ge Y (2018) Pyrrolnitrin is more essential than phenazines for *Pseudomonas chlororaphis* G05 in its suppression of *Fusarium graminearum*. Microbiol Res 215:55–64
Ji T, Lu A, Wu K (2017). Antisense RNA insert design for plasmid construction to knockdown target gene expression. Undergrad Methods Paper 1:7–15.
Jug U, Glavnik V, Kranjc E, Vovk I (2018) High-performance thin-layer chromatography and high-performance thin-layer chromatography-mass spectrometry methods for the analysis of phenolic acids. JPC-J Planar Chromat 31:13–22. https://doi.org/10.1556/1006.2018.31.1.2
Jung BK, Hong SJ, Park GS, Kim MC, Shin JH (2018). Isolation of Burkholderia cepacia JBK9 with plant growth-promoting activity while producing pyrrolnitrin antagonistic to plant fungal diseases. Applied Biological Chemistry 61:173–180
Karlenius TC, Tonissen KF (2010) Thioredoxin and cancer: a role for thioredoxin in all States of tumor oxygenation. Cancers 2(2):209–232
Kielkopf CL, Bauer W, Urbatsch IL (2021) Expressing cloned genes for protein production, purification, and analysis. Cold Spring Harb Protoc (2):pdb–top102129
King EO, Ward MK, Raney DE (1954) Two simple media for the demonstration of pyocyanin and fluorescein. J Lab Clin Med 44(2):301–307
Kõressaar T, Lepamets M, Kaplinski L, Raime K, Andreson R, Remm M (2018) Primer3_masker: integrating masking of template sequence with primer design software. Bioinformatics 34(11):1937–1938
Liu X, Liu L, Wang Y, Wang X, Ma Y, Li Y (2014) The study on the factors affecting transformation efficiency of *E. coli* competent cells. Cell 5:x106
Mehnaz S, Bauer JS, Gross H (2014) Complete genome sequence of the sugarcane endophyte *Pseudomonas aurantiaca* PB-St2, a disease-suppressive bacterium with antifungal activity toward the plant pathogen *Colletotrichum falcatum*. Genome Announc 27(21). https://doi.org/10.1128/genomeA.01108-13
Mohamed OM, Hussein AA, Badawi M, Mabel HE (2020) Antifungal activity of Pseudomonas fluorescence metabolites against some phytopathogenic fungi. Middle East J Appl Sci 10(02):158–168
Mozes-Koch R, Gover O, Tanne E, Peretz Y, Maori E, Chernin L, Sela I (2012) Expression of an entire bacterial Operon in plants. Plant Physiol 158(4):1883–1892
Navarro-Monserrat ED, Taylor CG (2023) T6SS: a key to *Pseudomonas's* success in biocontrol? Microorganisms 11(11): 2718. https://doi.org/10.3390/microorganisms11112718
Raj M, Patel SK, Sirisha L, Chaudhary R, Lal K, Kumar R (2020) Dynamic role of plant growth promoting rhizobacteria (PGPR) in agriculture. Int J Chem Stud 8(5):105–110. https://doi.org/10.22271/chemi.2020.v8.i5b.10284
Schmidt S, Blom JF, Pernthaler J, Berg G, Baldwin A, Mahenthiralingam E, Eberl L (2009) Production of the antifungal compound Pyrrolnitrin is quorum sensing-regulated in members of the *Burkholderia cepacia* complex. Environ Microbiol 11(6):1422–1437
Shahid I, Rizwan M, Baig DN, Saleem RS, Malik KA, Mehnaz S (2017) Secondary metabolites production and plant growth promotion by *Pseudomonas chlororaphis* and *P. aurantiaca* strains isolated from Cactus, cotton, and Para grass. J Microbiol Biotechnol 27(3):480–491
Shahid I, Han J, Hardie D, Baig DN, Malik KA, Borchers CH, Mehnaz S (2021) Profiling of antimicrobial metabolites of plant growth promoting *Pseudomonas* spp. Isolated from different plant hosts. 3 Biotech 11(2):48. https://doi.org/10.1007/s13205-020-02585-8
Sharma K, Lee SY, Ghiffary MR, Kim HU (2020) Engineering heterologous hosts for the enhanced production of non-ribosomal peptides. Biotechnol Bioprocess Eng 25(6):795–809. https://doi.org/10.1007/s12257-020-0080-z
Shishir MA, Hoq MM (2020) The exploitation of microbes: next generation global solution. Microb Bioact 3(1):106–109
Singh RN, Singh RP, Sharma A, Saxena AK (2016) Modeling of *PrnD* protein from *Pseudomonas fluorescens* RajNB11 and its comparative structural analysis with *PrnD* proteins expressed in *Burkholderia* and *Serratia*. Turk J Biol 40(3):623–633
Soliman SA, Khaleil MM, Metwally RA (2022) Evaluation of the antifungal activity of *Bacillus amyloliquefaciens* and *B. velezensis* and characterization of the bioactive secondary metabolites produced against plant pathogenic fungi. Biology 11(10):1390
van Pée KH and Ligon JM (2000). Biosynthesis of pyrrolnitrin and other phenylpyrrole derivatives by bacteria. Natural Product Reports 17(2):157–164.
Vasanthabharathi V, Jayalakshmi S (2018) Bioactive potential from marine sponge *Callyspongia diffusa* associated *Pseudomonas fluorescens* BCPBMS-1 and *Penicillium citrinum*. Microb Bioact 1(1):8–13. https://doi.org/10.25163/microbbioacts.1100202221300318
Yu Y, Chen L, Hao M, Wang L, Yu Z, Wang Y, Chi X, Feng Z, Cheng S, Ge Y (2021) A *TetR*/*AcrR* family regulator Pip induces phenazine biosynthesis but represses Pyrrolnitrin biosynthesis in biocontrol agent *Pseudomonas chlororaphis* G05. Biol Control 152:104448
Zameer M, Shahid I, Saleem RS, Baig DN, Zareen M, Malik KA, Mehnaz S (2025). Assessment of anticancer and antimicrobial potential of bioactive metabolites and optimization of culture conditions of Pseudomonas aurantiaca PB-St2 for High Yields. Journal of Microbiology and Biotechnology 35:e2311041.
Zhang B, Zhao H, Wu X, Zhang LQ (2020a) The oxidoreductase *Dsb*A1 negatively influences 2, 4-diacetylphloroglucinol biosynthesis by interfering the function of *Gcd* in *Pseudomonas fluorescens* 2P24. BMC Microbiol 20:1–9
Zhang J, Mavrodi DV, Yang M, Thomashow LS, Mavrodi OV, Kelton J, Weller DM (2020b) Pseudomonas synxantha 2–79 transformed with Pyrrolnitrin biosynthesis genes has improved biocontrol activity against soilborne pathogens of wheat and Canola. Phytopathology 110(5):1010–1017
Zhang L, Chen W, Jiang Q, Fei Z, Xiao M (2020c) Genome analysis of plant growth-promoting rhizobacterium Pseudomonas chlororaphis subsp. Aurantiaca JD37 and insights from comparison of genomics with three Pseudomonas strains. Microbiol Res 237:126483. https://doi.org/10.1016/j.micres.2020.126483
Zhang QX, Kong XW, Li SY, Chen XJ, Chen XJ (2020d) Antibiotics of *Pseudomonas protegens* FD6 are essential for biocontrol activity. Austral Plant Pathol 49:307–311